Hindawi
Journal of Nanomaterials
Volume 2023, Article ID 3599501, 10 pages
https://doi.org/10.1155/2023/3599501

Research Article

Effect of Different Ratios of *Mentha spicata* Aqueous Solution Based on a Biosolvent on the Synthesis of AgNPs for Inhibiting Bacteria

Motahher A. Qaeed,[1] Abdulmajeed Hendi,[2] Asad A. Thahe,[3] Saleh M. Al-Maaqar,[4] Abdalghaffar M. Osman,[5] A. Ismail,[6] A. Mindil,[1] Alharthi A. Eid,[1] Faisal Aqlan,[7] E. G. Al-Nahari,[8] Ahmed. S. Obaid,[9] Mohiuddin Khan Warsi,[10] Ala'eddin A. Saif,[1] and Ammar AL-Farga[10]

[1]*Department of Physics, Faculty of Science, University of Jeddah, Jeddah, Saudi Arabia*
[2]*Department of Physics, IRC Hydrogen and Energy Storage, King Fahd University of Petroleum and Minerals, Dhahran 31261, Saudi Arabia*
[3]*Department of Medical Physics, College of Applied Science, University of Fallujah, Fallujah, Iraq*
[4]*Faculty of Education, Department of Biology, Al-Baydha University, Al-Baydha, Yemen*
[5]*Department of Chemistry, IRC Hydrogen and Energy Storage, King Fahd University of Petroleum and Minerals, Dhahran 31261, Saudi Arabia*
[6]*Department of Physics, University of Hafr Al Batin, Hafr Al Batin 31991, Saudi Arabia*
[7]*Department of Chemistry, Faculty of Science, University of Jeddah, Jeddah, Saudi Arabia*
[8]*Department of Physics, Center of Excellence in Development of Non-Profit Organizations, King Fahd University of Petroleum and Minerals, Dhahran 31261, Saudi Arabia*
[9]*Department of Physics, College of Science, University of Anbar, Ramadi, Iraq*
[10]*Department of Biochemistry, Faculty of Science, University of Jeddah, Jeddah, Saudi Arabia*

Correspondence should be addressed to Saleh M. Al-Maaqar; salehalmagr@gmail.com

Received 22 September 2022; Revised 11 November 2022; Accepted 3 March 2023; Published 29 April 2023

Academic Editor: Haisheng Qian

Copyright © 2023 Motahher A. Qaeed et al. This is an open access article distributed under the Creative Commons Attribution License, which permits unrestricted use, distribution, and reproduction in any medium, provided the original work is properly cited.

Our work was devoted to studying the effect of different concentrations of *Mentha spicata* aqueous extract on the green synthesis of silver nanoparticles (AgNPs) in order to obtain the most effective of these concentrations for bacteria inhibitory activity. Different concentrations of the aqueous *M. spicata* extract (0.25, 0.50, 0.75, and 1.00 mM) were used as biological solvent to synthesize AgNPs by means of the reduction method. The crystal structure and morphology of the NPs were characterized UV–vis spectra, X-ray diffraction (XRD), and scanning electron microscopy (SEM). The inhibition effect of AgNPs on *Escherichia coli* was studied to determine the minimum inhibitory concentration (MIC). The dark yellow color of the *M. spicata* extract aqueous solution indicates the successful synthesis of the AgNPs. UV spectra of the NPs show a gradual increase in absorption with increasing concentration of aqueous *M. spicata* extract solution from 0.25 to 1.00 mM, accompanied by a shift in the wavelength from 455 to 479 nm along with a change in the nanoparticle size from 31 to 9 nm. The tests also showed a high activity of the particles against bacteria (*E. coli*) ranging between 15.6 and 62.5 μg/ml. From the AgNPs, it was confirmed that aqueous *M. spicata* extract is an effective biosolvent for the synthesis of different sizes of AgNPs according to the solvent concentration. The AgNPs also proved effectual for the killing of bacteria.

1. Introduction

Nanotechnology has opened a wide field that includes many scientific research that revolve around the synthesis, modification, and employment of particle structures whose dimensions are lower than 100 nm for numerous missions [1, 2]. The ratio between a large surface area to the volume of metallic NPs enables their application in many fields that include catalytic processes, biomedicine, and optoelectronics [3]. Recently, the

distinctive properties of Au, Ag, Pd, and Pt nanometals such as high stability and conductivity have been exploited [4]. Green synthesis method is favored because it is nontoxic and eco-friendly, low charge as no auxiliary reagents are needed, and very economical [5, 6]. These exceptional properties explain the increasing production of plant extracts for the purpose of synthesizing nanoparticles [7, 8].

The synthesis of nanoparticles using plants is of great advantage and benefits from other biological processes as it does not suffer from the problem of preserving the cell and is better than chemical methods because there is no toxicity as it is environmental friendly and less expensive [9]. One of the advantages of using green synthesis is that it contains a group of leaf extracts that act as biological vectors [10]. Alkaloids, flavonoids, and terpenoid compounds available in the extract have a potential to be responsible for reduction and stabilization of nanoparticles [11, 12]. One of the disadvantages of the green synthesis is that some organic compounds which are not toxic remain on the surface of the nanoparticles and appear in XRD measurements [13]. Recently, AgNPs have been of paramount importance as they have a great role in the fight against cancer in the medical field [14], antioxidant [10], and antibacterial [1, 15] due to their better photolysis efficiency compared with organic dyes [16]. Various biological precursors such as various parts of plants, plant by-products, and algae are utilized in the green synthesis of AgNPs [16]. The leaf aqueous extract plays a significant role in the stability of AgNPs through surface interaction with the nanoparticles and then capping to prevent the aggregation of the synthesized AgNPs. Many plant extracts used for this purpose such us *Limoniaacidissima* [17], *Indigofera tinctoria* [18], *Zingiberofficinale* [19], *Prosopic juliflora* [20], *Lagerstroemia speciosa* [21], *Azadirachaindica* [22], *Avicennia marina* [23], and *Bauhinia purpurea* [24], have shown great ability to inhibit the action of bacteria.

Synthesis of AgNPs formed using green synthesis: [25–35], and various chemical and green synthesis methods [36, 37], biomolecules including DNA [38–42], protein [43–45], enzyme [26], protein [43–45], and plant extracts [26, 46–49] with their biological properties [50–52].

The motive of this work is to exploit the large availability of mint plants in the city of Jeddah, Kingdom of Saudi Arabia, in the production of different sizes of AgNPs by adding variable proportions of the aqueous extract of mint to a fixed value of silver nitrate with time and constant temperature in order to reduce the cost, as the green synthesis is environmental friendly and safer in terms of health, and studying the effect of different sizes of silver nanoparticles on the inhibition of bacterial growth. In the future it is possible to manufacture liquid materials that are used to sterilize places where bacterial infection spreads.

Our study aims to define the impact of different ratios of aqueous extract of *Mentha spicata* with a fixed percentage of silver nitrate ($AgNO_3$) solution on the size of AgNPs. This study also explores the impact of *M. spicata* extract on AgNPs via a green synthesis on inhibiting bacteria growth.

2. Methodology

2.1. Materials. The materials used for AgNPs synthesis include *M. spicata* leaves, filter papers, silver nitrate, distilled water, and glass substrates. A number of researchers studied the compounds of *M. spicata* oils, where in the composition of the essential oil of *M. spicata*, about 34 compounds were identified, representing 99.9% of the total compounds [53] as the main compound Carvone and the secondary compounds limonene and 1,8-senol [54–56]). In addition, it produces a large group of natural terpenoids called menthol ($C_{10}H_{20}O$) found in the essential oils of the mint family (Mentha spp.) [57]. The diversity in the proportions of the contents of mint from one country to another is due to several factors, including humidity, agricultural conditions, temperature, photoperiod, and others [53].

2.2. Prepare the Plant Extract. The leaves of *M. spicata* were collected, washed, dehydrated, and grounded until a fine powder was achieved. Ten grams of *M. spicata* powder with 100 ml of distilled water was mixed in a glass flask. The contents in the glass was stirred using a magnetic stirrer at 27°C for 1 hr. Then, the mixture was subsequently filtered to obtain the aqueous extract of *M. spicata* plant. The extract was then dried using a dryer. Afterward, 1 g of dry extract and 100 ml of distilled water were mixed for 15 min until it completely dissolved to obtain an original stock solution with a concentration of 10,000 ppm. From this original solution, other concentrations were prepared.

2.3. Preparation of Silver Nitrate Solution. Several $AgNO_3$ solutions were prepared. First, 0.179 g of $AgNO_3$ with 100 g of distilled water was mixed to obtain a concentration of 1 mM. Second, 1 ml of $AgNO_3$ and 100 ml of distilled water were mixed until completely dissolved. Third, 5 ml of $AgNO_3$ and 1 ml of plant extract were mixed at room temperature until the color of the liquid became clear, which indicates the formation of AgNPs.

2.4. Preparation of Glass Substrates. The glass substrates were cut into lengths of $2.5 \times 2.5\ cm^2$, which were then washed with distilled water and placed in an ultrasonic device for 15 min. Afterward, the glass substrates were immersed in acetone (purity of 99%) to remove impurities on the surface. The substrates were then returned to the ultrasonic device for 10 min.

2.5. Drop Casting. To precipitate the AgNPs on the substrate, the $AgNO_3$ solution was placed in an ultrasonic device to ensure homogeneity, and then the liquid was placed in the dropper. The solution was distilled onto a heated substrate at 50°C to dry.

2.6. Characterization. The prepared samples were characterized by various techniques. The optical properties of the samples were analyzed by recording the diffuse reflectance spectra using the Cary Series UV–Vis-NIR Spectrophotometer-Agilent Technologies. The structural properties were examined by an X-ray diffractometer (Rigaku Ultima IV) equipped

with Cu Kα X-ray source ($\lambda = 0.15406$ nm). The scan rate and acquisition 2θ range were 0.5 °/min and 20° to 90°, respectively, and the morphology of the prepared samples were inspected by the field emission scanning electron microscopy (FESEM, Lyra 3).

2.7. Antibacterial Activity of AgNPs

2.7.1. The Diffusion Measurement of Agar Well. To prepare the investigation of Agar well diffusion, *Escherichia coli* (10^6 colony-forming units/ml) was injected to Mueller Hinton Agar (MHA) media. For each cultivation dishes, six 6 mm-sized holes were cut out by means of a sterile glass pipette. Various concentrations of 70 μl of AgNPs were prepared and poured into the holes, a negative control was utilized for the sterilized distilled water (SDW). Afterward, incubation of the dishes was done for 24 hr at 37°C. The inhibition region was calculated as the mean ± standard deviation (SD) of triplicate investigations [58].

2.7.2. Determining the Minimum Inhibitory Concentrations of AgNPs (MIC). To assess their capacity to prevent bacterial growth, the minimum inhibitory concentrations (MICs) of AgNPs were using micro-broth dilution inspection by means of a 96-well microtiter dish. The MICs were determined utilizing the microdiluted broth technique according to NCCLS [59]. The incubation of samples was done for 24 h at 37°C. After the incubation procedure, 10 μl Resazurin sodium salt dye (R7017 Sigma–Aldrich) was added to every well [60]. Column 12, which holds media as a negative control, only verifies the absence of contamination on the plate in the course of preparing the dish. Column 1 is a positive control that contains cultured strain only with media, whereas Column 2–10 contains the serial dilution of the AgNPs with media.

2.7.3. Estimation of Minimal Bactericidal Concentration for AgNPs Synthesized by Different Aqueous Mentha spicata Solutions. The lowest concentration of AgNPs at which the inoculated bacteria was destroyed is referred as minimal bactericidal concentration (MBC). The determination involves spreading 10 μl of medium from the microplate contents of MIC that displayed no bacterial growth, which were inoculated again, on nutritive agar dishes. Then for 24 hr at 37°C the dishes awere incubated. The first well with colony counts of less than 5 is considered negative for growth and described as the MBC [60].

2.7.4. Time-Killing Kinetics. To obtain the time-killing kinetics, the highest MIC of AgNPs and Augmentin for bacterial strain was measured in Muller–Hinton broth. The cultures were subjected to aerobic incubation at 37°C. Afterward, to determine the antibiotic concentrations, the Augmentin and AgNPs solutions were added to the well at 0, 2, 4, 6, 8, 10, 12, and 24 hr followed by incubation of AgNPs and antibiotic solution into the well. Utilizing sterilized loop, samples of 0.001 μl from the cultures were collected sterilely and streaked uniformly on blood agar dish and subsequently incubated at 37°C ± 1 for 24 hr. Afterward, the bacterial colonies in the cultures were counted by the means of a plate counter [61].

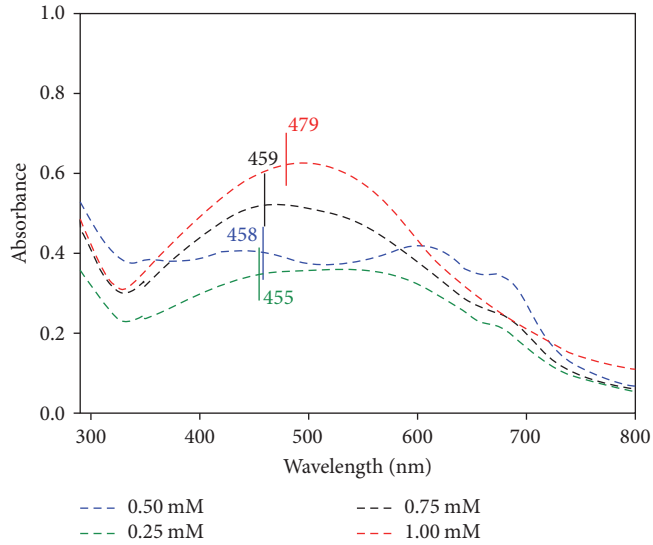

FIGURE 1: UV–vis spectra of AgNPs biosynthesized using *Mentha spicata* aqueous plant extracts.

3. Results and Discussion

The extract is prepared by sorting, washing, and drying the plant parts. The plant extract possesses various biomolecules such as terpenoids, phenolic acids, sugars, alkalis, polyphenols, alkalis, etc., which play a major role in reducing and stabilizing silver nanoparticles. It plays a large role in the size of the plant extract used and the size of silver ions in addition to other parameters such as temperature and time. These biological compounds reduce $AgNO^3$ to Ag^+. Then, electrons are supposed to be derived from dehydrogenation of acids and alcohols (catechol) in hydrophytes, from keto to enol, to create Ag^0 [62, 63].

3.1. UV–Vis Spectra of AgNPs. In AgNPs, the valence bond is very close to the conduction band, causing the electrons to move very freely, thus raising the surface plasmon resonance (SPR) absorption [64, 65], which leads to resonant oscillation of the AgNPs electrons with the incident light [66]. This results in a dipole oscillation of all electrons on the surface with the same phase. The resonance occurs between the absorption and extinction frequency at different values, as shown in Figure 1, which is attributable to the difference in the size of the particles [67, 68]. Figure 1 shows the formation of AgNPs caused by the reduction process; its formation is conclusively indicated in the presence of the solution color and its gradation from light yellow to dark yellow. The negative surface charges of the suspended NPs prevent their aggregation according to Coulomb's law. In Figure 1, it appears that the saturated reaction resulted from the addition of different proportions of aqueous extract of *M. spicata* plant. The UV spectra of the NPs show a gradient of increasing absorption with the concentration of the extract, with accompanition of a shift in the wavelength from 455 to 479 nm. This is due to the varying sizes and shapes of the particles as well as the availability of phytochemical compounds in the extract [69, 70]. The characteristic peaks of

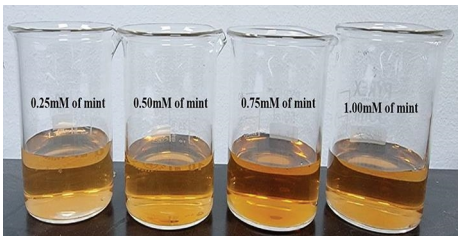

Figure 2: Color gradient in AgNPs liquid.

these compounds are discernible in the XRD spectra. As observed, the full-width at half maximum (FWHM) increased with extract concentration. The increase in intensity indicates a decrease in the bandwidth [71].

The spectrum also indicates an incensement in the concentration of *M. spicata* extract works to control the reduction process due to the phytochemical compounds available in the leaves, which subsequently increases the concentration of AgNPs and thereby increases the intensity of absorption. Thus, the increased concentration of *M. spicata* extract concomitantly increases the number of vital compounds responsible for Ag^+ conversion to Ag^0. The absence of combined bands in Figure 1 indicates the nonaggregation of AgNPs [67].

It appears that the color of the aqueous AgNPs changed from light yellow to dark yellow, which is because of the different sizes of the synthesized NPs (Figure 2). As observed in Figure 2, higher the percentage of *M. spicata* extract, higher the antioxidants, which work to continue the reaction and increase the concentration of particles, thus increasing the intensity of the UV–vis spectra [72].

3.2. XRD Measurement. The X-ray diffraction measurements of AgNPs synthesized by *M. spicata* leaf extract are presented in Figure 3. The XRD spectra show the Bragg reflections represented by the fcc structure. The XRD was presented as a function of the extract concentration while the sample of 0.5 mM of *M. spicata* extract concentrations appear different for the control group; the reason for this is the presence of cracks on the surface of the sample or perhaps the presence of a few defects or contaminations on the surface during the deposition process. The discernible peaks at 2θ values of 37.80° and 77.1°, which were reflected from the (111) and (311) planes, respectively, matches with the study by Ahmad et al. [73] and Jemal et al. [74]. The (111) and (311) crystal phases were observed in the samples synthesized with 0.25 and 0.50 mM of *M. spicata* extract concentrations, while only (111) phase was identified for the sample synthesized with 0.75 and 1 mM *M. spicata* extract concentrations.

The particle sizes of AgNPs calculated via Scherer formula are presented in the Table 1 [13]. The highest intensity XRD peak was observed at 37.89°, denoting (111) crystal phase. This indicates that most of the synthesized AgNPs accumulate and grow at the (111) plane, while the remainder of NPs grow in the direction of the (311) plane [73]. As deduced from the table, higher the percentage of *M. spicata* aqueous extract, lower the percentage of Ag ions in the *M. spicata* aqueous solution, resulting in reduced the NPs size [75]. As shown in Figure 3, the sample synthesized with 1.00 mM aqueous *M. spicata* solution has the lowest intensity peak, due to its relatively smaller particle size compared with the other samples. This confirms that the size and aggregation of AgNPs are following the concentration of the *M. spicata* solution. This is corroborated by the narrow XRD peak and SEM image (Figure 5) of the sample. Two unspecified peaks were also observed at 32.25 and 46.21, which may be attributable to the bio-organic compounds that remain attached to the surface of the NPs or possibly because of the availability of organic compounds in *M. spicata* leaf extract [13, 76]. Jeeva et al. [77] reported that the XRD peaks that appear at 32.28°, 46.28°, 54.83°, 67.47°, and 76.69° denote phytochemical compounds in leaf extracts [77].

3.3. Scanning Electron Microscopy (SEM) Measurement. In this part, the AgNPs morphology of the sample with the smallest nanoparticle size and least aggregation (i.e., sample synthesized with 0.25 mM *M. spicata* extract) was investigated using SEM. It is clear that the AgNPs form clusters (Figure 4(a)) of different dimensions and shapes (Figure 4(b)) and are less than 100 nm. This strongly confirms that *M. spicata* extract is effective as a solvent in the formation of AgNPs. The histogram distribution of the focused area presented in Figure 4(c) indicates that the AgNPs sizes generally vary from 40 to 50 nm.

3.3.1. Antibacterial Test using Agar Diffusion Assay. Antibacterial impact of AgNPs was determined for one species of Gram-negative pathogen, *E. coli* ATCC 35218. The results for the well diffusion test, MBC, and MIC were presented separately of AgNPs. For well diffusion test, the clear zone around the AgNPs well suggests that the AgNPs exhibit antibacterial activity against the growth of the Gram-negative pathogen. The bacteria inhibition zones against *E. coli* ATCC 35218 vary from 12 ± 0.5 mm to 15 ± 0.5 mm for *M. spicata* extract concentration range of 0.25–1.00 mM, successively, as shown in Figure 5. The findings of this study is consistent with previous reports [60].

3.3.2. Antibacterial Test using MIC and MBC. The well diffusion test is a preliminary procedure for screening the antibacterial activity of an antimicrobial agent, while determination of MIC value is a more detailed evaluation. By serial dilution, the antibacterial agent with a low concentration that resists the growth and reproduction of bacteria is known as MIC. On the other hand, the antibacterial agent with lowest concentration that is needed to kill bacteria is known as MBC. As shown in Figure 6, the AgNPs have MIC values against the pathogen (*E. coli*) between 15.36 and 62.5 μg/ml for aqueous *M. spicata* extract concentration range of 0.25–1.00 mM. The MBC values for *E. coli* ranged between 31.25 and 125 μg/ml for *M. spicata* extract concentration of 0.25–1.00 mM, as shown in Table 2. These findings are consistent with previous studies [60].

3.3.3. Time-Killing Kinetics. The time-killing curves revealed that the synthesized AgNPs are less effective than Augmentin Table 3. Moreover, according to MIC test, the sample prepared with 1.00 mM *M. spicata* aqueous solution was the most effective. After the incubation period of 6–12 hr, all the bacterial cells were totally destroyed. However, it was

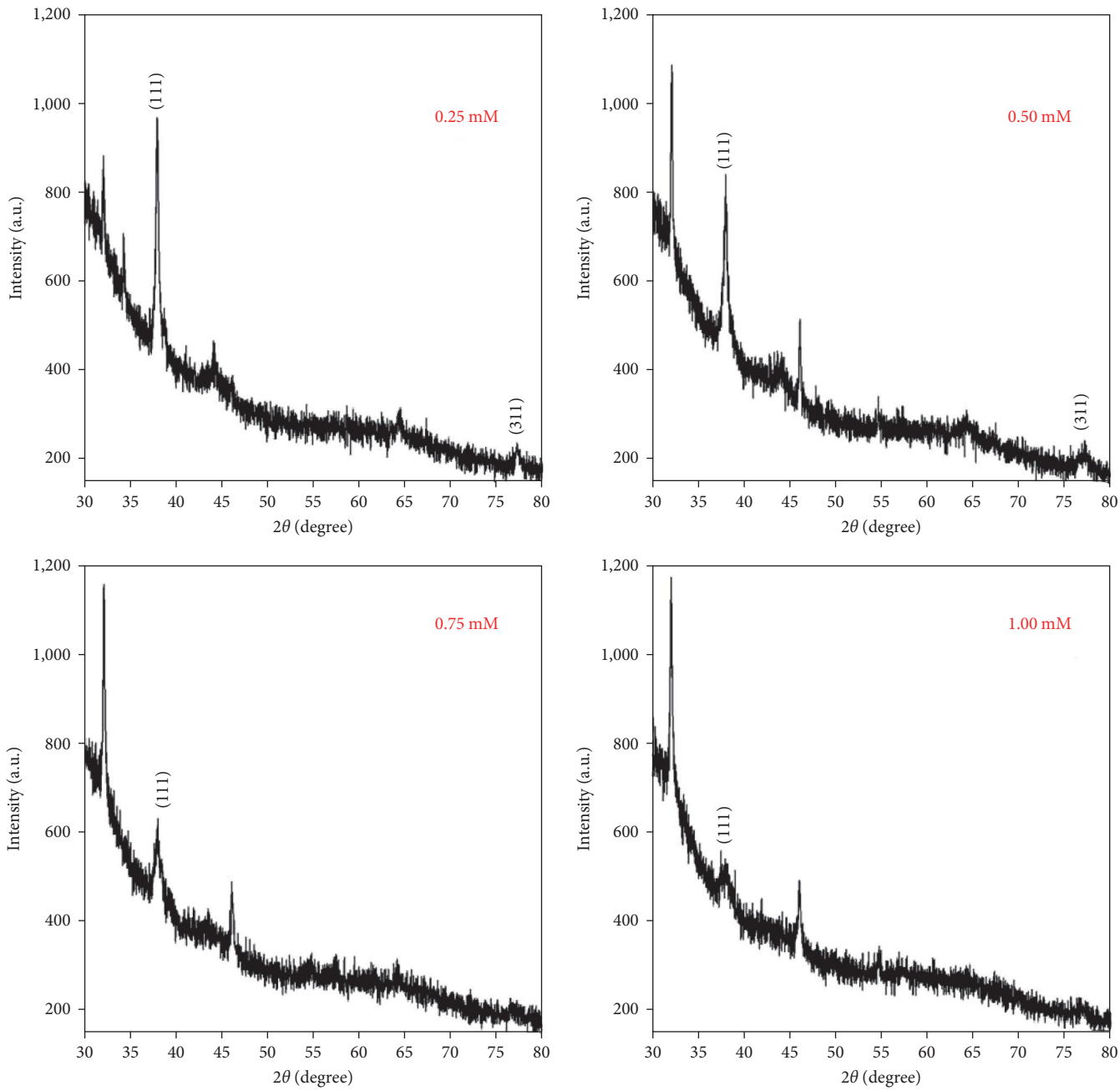

Figure 3: XRD of AgNPs biosynthesized using *Mentha spicata* aqueous plant extracts.

Table 1: The size of AgNPs biosynthesized using *Mentha spicata* aqueous plant extracts.

Sample (mM)	2θ (°)	FWHM (°)	d (angle)	Phase name	AgNPs size (nm)	Average size (nm)
0.25	37.88	0.295	2.374	(1,1,1)	29.7	31.1
	77.13	0.327	1.235	(3,1,1)	32.5	
0.50	37.88	0.412	2.373	(111)	21.3	15.8
	77.17	1.031	1.236	(3,1,1)	10.3	
0.75	37.83	0.886	2.378	(111)	9.9	9.9
1.00	37.85	0.62	2.377	(111)	9.1	9.1

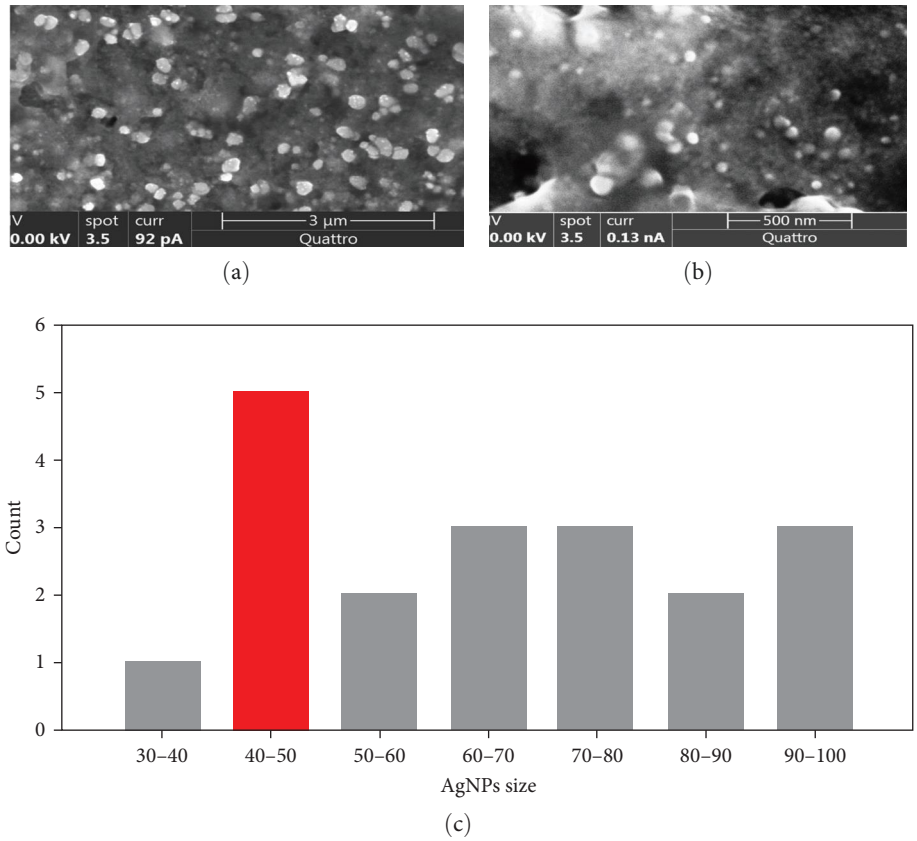

Figure 4: SEM image of AgNPs prepared by 0.25 mM of aqueous *Mentha spicata* solution.

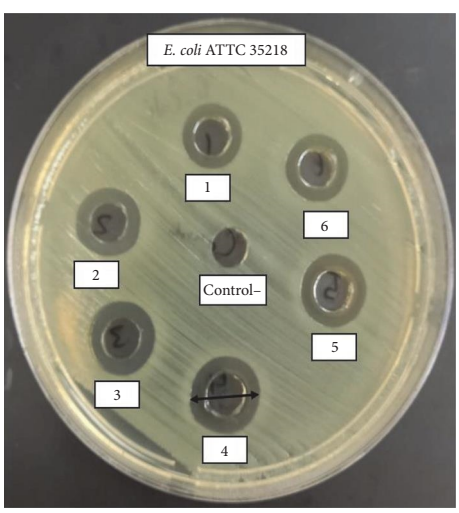

Figure 5: Inhibition zone (mm) of AgNPs using *Mentha spicata* aqueous plant extracts at different concentrations by Agar well diffusion method against *Escherichia coli* ATCC 35218. The zone of inhibitions are, respectively, 12 ± 0.5, 13.5 ± 0.5, 14 ± 0.5, 15 ± 0.5, 14 ± 0.5, 13 ± 0.5. Key: 1 : 0.0625, 2 : 0.125, 3 : 0.250, 4 : 0.5, 5 : 0.75, 6 : 1 mM.

observed that the bacteria density for strain increased rapidly to a peak of 5×10^5 bacteria/ml. For the sample prepared with 1.00 mM *M. spicata* aqueous solution, it was noted that after 6 hr of incubation, the pathogenic bacteria were

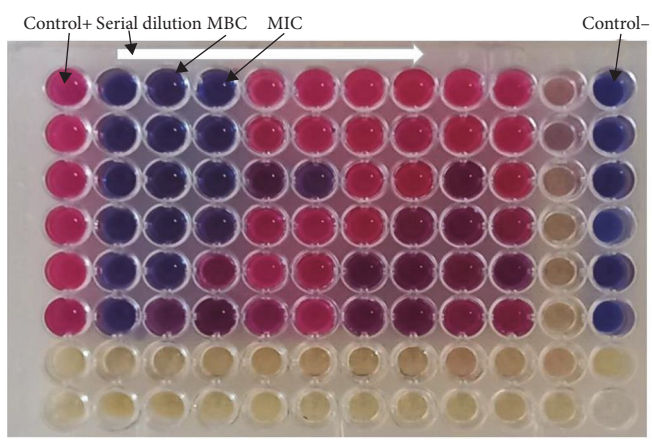

Figure 6: Determination of MIC and MBC NPs against pathogenic bacteria (*Escherichia coli*) using Resazurin dye. The rows A–G each represent samples from one to six with pathogenic bacterium (*Escherichia coli*).

Table 2: MIC and MBC values of AgNPs prepared with different aqueous solution of *Mentha spicata* against the pathogen (*E. coli*).

	0.25 mM	0.50 mM	0.75 mM	1.00 mM
MIC (μg/ml)	15.63	31.25	46.88	62.5
MBC (μg/ml)	31.25	62.5	93.75	125

Table 3: Time-killing curve for *Escherichia coli* ATCC 35218 of *Mentha spicata* and Augmentin as control.

Time (hr)	Normal growth of *E. coli*	Mentha extract	Augmentin (as control)
0	5×10^5	5×10^5	5×10^5
2	6.4×10^5	4.5×10^5	3×10^5
4	8.6×10^5	3.2×10^5	1.8×10^5
6	9×10^5	2.8×10^5	$8.\times10^4$
8	1×10^6	1.6×10^5	7×10^4
10	1.05×10^6	1×10^4	0
12	1.18×10^6	0	0
24	1.2×10^6	0	0

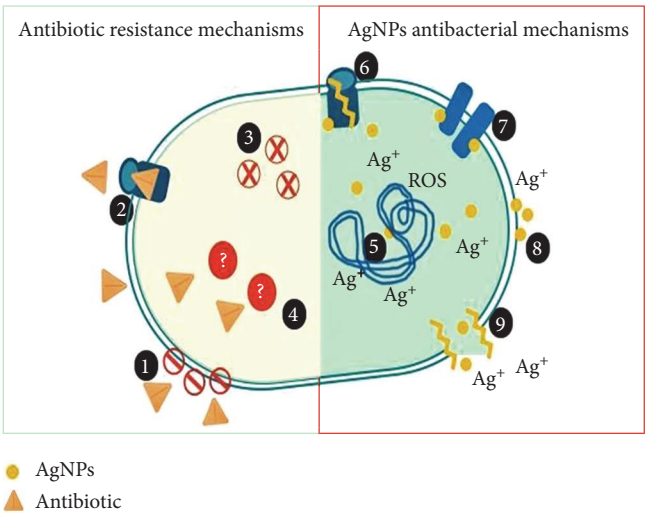

Figure 7: Comparative scheme between resistance mechanisms in bacteria and antibacterial mechanisms of AgNPs. Antibiotic resistance mechanisms include (1) permeation barriers, (2) efflux pumps, (3) inactivation of antibiotic, and (4) structural changes in antibiotic targets (represented as "?") avoiding its recognition. On the other side, AgNPs antibacterial mechanisms includes (6) alteration of efflux pumps, (7) disruption of membrane proteins and electron transport chains, (8) accumulation in membrane affecting permeation, (9) disruption of membrane and leakage of intracellular content, and (5) interaction and damage in DNA. A similar figure was published in the study by Bruna et al. [79].

killed, while during 12–24 hr, the growth of bacteria was zero. This is compatible with the abovementioned tests. This phenomenon is explained as follows: the 1 mM of *M. spicata* extract solution results in smaller AgNPs, which enables their penetration through the cell wall of bacteria and destroys them completely, whereas the larger particles penetrate the cell wall of bacteria with difficulty [78]. One of the common and important applications of AgNPs is that they are highly efficient in inhibiting Gram-positive and negative bacteria. It depends on physical properties such as surface morphology and size that enable it to travel through the wall of the cell and membranes into the cell [79]. AgNPs inhibit the action of bacteria through three essential stages associated with multiple mechanism shown in Figure 7. In the first stage, the AgNPs are supposed to work at the membrane level, where they have the ability to break through the outer permeable membrane, while the inner membrane collapses upon the adhesion of AgNPs, which in turn leads to destabilization and increased membrane permeability, so the cell content leaks outside, resulting into cell damage and death [80, 81]. The second stage likely involves the interaction of AgNPs with the phosphorous and sulfur groups available in the cell-like proteins and DNA, which changes their functions and structure. Alternatively, the interaction with the thiol group in the enzymes leads the change in the respiratory system in the inner membrane, which then leads to the formation of free radicals and reactive oxygen species, resulting in injury to the machinery intracellular. Third stage is initiated when Ag ions are released from the NPs, and this depends on their size and charge. This will change the metabolic pathway [82, 80]. It was clear from the measurements of MIC that the inhibition of bacterial action is strongly dependent on the size of particles, where the majority of the surface that becomes in direct touch with the cell of bacteria results from the smaller size silver nanoparticles [82]. The researchers also noted that smaller the size of AgNPs, higher the stimulation of the reactive oxygen species, which increases the killing effect on *E. coli* [83]. It is also noted that the charged particles have a relatively high activity against bacteria of smaller sizes, as they have a greater solubility in different media, which accompanies the liberation of positive Ag ions; and here, the electrical attraction between the positive charge of AgNPs and the negative charge of bacterial cell strengthens this interaction [84, 85].

4. Conclusion

AgNPs were successfully prepared in less costly, environmental friendly, and less toxic conditions using the green synthesis method. Different proportions of aqueous extract of *M. spicata* acted as reducing agent to function as biosolvent. The sizes of the AgNPs varied from 30 to 9 nm with increasing concentration of aqueous extract from 0.25 to 1.00 mM, which confirms the possibility of tuning the size of AgNPs during its synthesis. The spherical-shaped AgNPs exhibited an absorption peak in the visible spectrum. The smallest size and least aggregation of AgNPs were achieved at *M. spicata*-extract concentration of 1 mM. At this concentration, the AgNPs were able to penetrate the wall of bacterial cell and destroy it completely. The AgNPs antibacterial activity against *E. coli* ATCC 35218 was significant. Based on the results, AgNPs can be considered as antibacterial agents

against pathogenic microorganisms. The use of AgNPs in various fields, such as medical devices and antimicrobial systems, could lead to beneficial discoveries.

Data Availability

The data used to support the findings of this study are included within the article.

Conflicts of Interest

The authors declare that they have no conflicts of interest.

Acknowledgments

The authors thank the University of Jeddah for providing facilities for the production of this work.

References

[1] Y. K. Mohanta, S. K. Panda, R. Jayabalan, N. Sharma, A. K. Bastia, and T. K. Mohanta, "Antimicrobial, antioxidant and cytotoxic activity of silver nanoparticles synthesized by leaf extract of *Erythrina suberosa* (Roxb.)," *Frontiers in Molecular Biosciences*, vol. 4, Article ID 14, 2017.

[2] G. Sathishkumar, C. Gobinath, K. Karpagam, V. Hemamalini, K. Premkumar, and S. Sivaramakrishnan, "Phyto-synthesis of silver nanoscale particles using *Morinda citrifolia* L. and its inhibitory activity against human pathogens," *Colloids and Surfaces B: Biointerfaces*, vol. 95, pp. 235–240, 2012.

[3] D. Baruah, R. N. S. Yadav, A. Yadav, and A. M. Das, "Alpinia nigra fruits mediated synthesis of silver nanoparticles and their antimicrobial and photocatalytic activities," *Journal of Photochemistry and Photobiology B: Biology*, vol. 201, Article ID 111649, 2019.

[4] X. Zhang, H. Sun, S. Tan, J. Gao, Y. Fu, and Z. Liu, "Hydrothermal synthesis of Ag nanoparticles on the nanocellulose and their antibacterial study," *Inorganic Chemistry Communications*, vol. 100, pp. 44–50, 2019.

[5] B. A. de Marco, B. S. Rechelo, E. G. Tótoli, A. C. Kogawa, and H. R. N. Salgado, "Evolution of green chemistry and its multidimensional impacts: a review," *Saudi Pharmaceutical Journal*, vol. 27, no. 1, pp. 1–8, 2019.

[6] P. M. Falcone and M. Hiete, "Exploring green and sustainable chemistry in the context of sustainability transition: the role of visions and policy," *Current Opinion in Green and Sustainable Chemistry*, vol. 19, pp. 66–75, 2019.

[7] S. M. Gamboa, E. R. Rojas, V. V. Martínez, and J. Vega-Baudrit, "Synthesis and characterization of silver nanoparticles and their application as an antibacterial agent," *International Journal of Biosensors & Bioelectronics*, vol. 5, no. 5, pp. 166–173, 2019.

[8] P. Vaid, P. Raizada, A. K. Saini, and R. V. Saini, "Biogenic silver, gold and copper nanoparticles–A sustainable green chemistry approach for cancer therapy," *Sustainable Chemistry and Pharmacy*, vol. 16, Article ID 100247, 2020.

[9] R. Veerasamy, T. Z. Xin, S. Gunasagaran et al., "Biosynthesis of silver nanoparticles using mangosteen leaf extract and evaluation of their antimicrobial activities," *Journal of Saudi Chemical Society*, vol. 15, no. 2, pp. 113–120, 2011.

[10] M. Rai, A. Yadav, and A. Gade, "Silver nanoparticles as a new generation of antimicrobials," *Biotechnology advances*, vol. 27, no. 1, pp. 76–83, 2009.

[11] M. Dubey, S. Bhadauria, and B. S. Kushwah, "Green synthesis of nanosilver particles from extract of Eucalyptus hybrida (safeda) leaf," *Digest Journal of Nanomaterials and Biostructures*, vol. 4, no. 3, pp. 537–543, 2009.

[12] J. Huang, Q. Li, D. Sun et al., "Biosynthesis of silver and gold nanoparticles by novel sundried *Cinnamomum camphora* leaf," *Nanotechnology*, vol. 18, no. 10, Article ID 105104, 2007.

[13] V. Kumar and S. K. Yadav, "Plant-mediated synthesis of silver and gold nanoparticles and their applications," *Journal of Chemical Technology & Biotechnology*, vol. 84, no. 2, pp. 151–157, 2009.

[14] Z. A. Ratan, M. F. Haidere, M. Nurunnabi et al., "Green chemistry synthesis of silver nanoparticles and their potential anticancer effects," *Cancers*, vol. 12, no. 4, Article ID 855, 2020.

[15] A. Pugazhendhi, D. Prabakar, J. M. Jacob, I. Karuppusamy, and R. G. Saratale, "Synthesis and characterization of silver nanoparticles using *Gelidium amansii* and its antimicrobial property against various pathogenic bacteria," *Microbial pathogenesis*, vol. 114, pp. 41–45, 2018.

[16] M. S. Samuel, E. Selvarajan, T. Mathimani et al., "Green synthesis of cobalt-oxide nanoparticle using jumbo Muscadine (*Vitis rotundifolia*): characterization and photo-catalytic activity of acid Blue-74," *Journal of Photochemistry and Photobiology B: Biology*, vol. 211, Article ID 112011, 2020.

[17] R. S. Patil, M. R. Kokate, and S. S. Kolekar, "Bioinspired synthesis of highly stabilized silver nanoparticles using *Ocimum tenuiflorum* leaf extract and their antibacterial activity," *Spectrochimica Acta Part A: Molecular and Biomolecular Spectroscopy*, vol. 91, pp. 234–238, 2012.

[18] R. Vijayan, S. Joseph, and B. Mathew, "*Indigofera tinctoria* leaf extract mediated green synthesis of silver and gold nanoparticles and assessment of their anticancer, antimicrobial, antioxidant and catalytic properties," *Artificial Cells, Nanomedicine, and Biotechnology*, vol. 46, no. 4, pp. 861–871, 2018.

[19] S. Mathew, A. Prakash, and E. K. Radhakrishnan, "Sunlight mediated rapid synthesis of small size range silver nanoparticles using *Zingiber officinale* rhizome extract and its antibacterial activity analysis," *Inorganic and Nano-Metal Chemistry*, vol. 48, no. 2, pp. 139–145, 2018.

[20] G. Arya, R. M. Kumari, N. Gupta, A. Kumar, R. Chandra, and S. Nimesh, "Green synthesis of silver nanoparticles using *Prosopis juliflora* bark extract: reaction optimization, antimicrobial and catalytic activities," *Artificial Cells, Nanomedicine, and Biotechnology*, vol. 46, no. 5, pp. 985–993, 2018.

[21] K. Basumatary, P. Daimary, S. K. Das et al., "Lagerstroemia speciosa fruit-mediated synthesis of silver nanoparticles and its application as filler in agar based nanocomposite films for antimicrobial food packaging," *Food Packaging and Shelf Life*, vol. 17, pp. 99–106, 2018.

[22] M. Mankad, G. Patil, D. Patel, P. Patel, and A. Patel, "Comparative studies of sunlight mediated green synthesis of silver nanoparaticles from *Azadirachta indica* leaf extract and its antibacterial effect on *Xanthomonas oryzae* pv. oryzae," *Arabian Journal of Chemistry*, vol. 13, no. 1, pp. 2865–2872, 2020.

[23] V. Abdi, I. Sourinejad, M. Yousefzadi, and Z. Ghasemi, "Mangrove-mediated synthesis of silver nanoparticles using native *Avicennia marina* plant extract from southern Iran," *Chemical Engineering Communications*, vol. 205, no. 8, pp. 1069–1076, 2018.

[24] S. Chinnappan, S. Kandasamy, S. Arumugam, K.-K. Seralathan, S. Thangaswamy, and G. Muthusamy, "Biomimetic synthesis of silver nanoparticles using flower extract of *Bauhinia purpurea* and its antibacterial activity against clinical pathogens," *Environmental Science and Pollution Research*, vol. 25, pp. 963–969, 2018.

[25] R. Ceylan, A. Demirbas, I. Ocsoy, and A. Aktumsek, "Green synthesis of silver nanoparticles using aqueous extracts of three Sideritis species from Turkey and evaluations bioactivity potentials," *Sustainable Chemistry and Pharmacy*, vol. 21, Article ID 100426, 2021.

[26] S. Ekrikaya, E. Yilmaz, C. Celik et al., "Investigation of ellagic acid rich-berry extracts directed silver nanoparticles synthesis and their antimicrobial properties with potential mechanisms towards *Enterococcus faecalis* and *Candida albicans*," *Journal of Biotechnology*, vol. 341, pp. 155–162, 2021.

[27] Z. Karaagac, O. T. Gul, N. Ildiz, and I. Ocsoy, "Transfer of hydrophobic colloidal gold nanoparticles to aqueous phase using catecholamines," *Journal of Molecular Liquids*, vol. 315, Article ID 113796, 2020.

[28] Z. Karaagac, I. Onal, N. Ildiz, and I. Ocsoy, "Simultaneous use of phenylboronic acid as a phase transfer agent and targeting ligand for gold nanoparticles," *Materials Letters*, vol. 280, Article ID 128561, 2020.

[29] I. Ocsoy, A. Demirbas, E. S. McLamore, B. Altinsoy, N. Ildiz, and A. Baldemir, "Green synthesis with incorporated hydrothermal approaches for silver nanoparticles formation and enhanced antimicrobial activity against bacterial and fungal pathogens," *Journal of Molecular Liquids*, vol. 238, pp. 263–269, 2017.

[30] I. Ocsoy, M. Temiz, C. Celik, B. Altinsoy, V. Yilmaz, and F. Duman, "A green approach for formation of silver nanoparticles on magnetic graphene oxide and highly effective antimicrobial activity and reusability," *Journal of Molecular Liquids*, vol. 227, pp. 147–152, 2017.

[31] B. S. Rajan, M. A. S. Balaji, A. B. M. A. Noorani, M. U. H. Khateeb, P. Hariharasakthisudan, and P. A. Doss, "Tribological performance evaluation of newly synthesized silane treated shell powders in friction composites," *Materials Research Express*, vol. 6, no. 6, Article ID 065317, 2019.

[32] H. Shi, X. Chen, L. Li et al., "One-pot and one-step synthesis of bioactive urease/$ZnFe_2O_4$ nanocomposites and their application in detection of urea," *Dalton Transactions*, vol. 43, no. 24, pp. 9016–9021, 2014.

[33] S. Some, O. Bulut, K. Biswas et al., "Effect of feed supplementation with biosynthesized silver nanoparticles using leaf extract of *Morus indica* L. V1 on *Bombyx mori* L. (Lepidoptera: Bombycidae)," *Scientific Reports*, vol. 9, Article ID 14839, 2019.

[34] A. Strayer, I. Ocsoy, W. Tan, J. B. Jones, and M. L. Paret, "Low concentrations of a silver-based nanocomposite to manage bacterial spot of tomato in the greenhouse," *Plant Disease*, vol. 100, no. 7, pp. 1460–1465, 2016.

[35] I. S. Unal, A. Demirbas, I. Onal, N. Ildiz, and I. Ocsoy, "One step preparation of stable gold nanoparticle using red cabbage extracts under UV light and its catalytic activity," *Journal of Photochemistry and Photobiology B: Biology*, vol. 204, Article ID 111800, 2020.

[36] I. Ocsoy, B. Gulbakan, T. Chen et al., "DNA-guided metal-nanoparticle formation on graphene oxide surface," *Advanced Materials*, vol. 25, no. 16, pp. 2319–2325, 2013.

[37] L. Peng, M. You, C. Wu et al., "Reversible phase transfer of nanoparticles based on photoswitchable host–guest chemistry," *ACS Nano*, vol. 8, no. 3, pp. 2555–2561, 2014.

[38] T. Chen, I. Öçsoy, Q. Yuan et al., "One-step facile surface engineering of hydrophobic nanocrystals with designer molecular recognition," *Journal of the American Chemical Society*, vol. 134, no. 32, pp. 13164–13167, 2012.

[39] N. Ma, E. H. Sargent, and S. O. Kelley, "One-step DNA-programmed growth of luminescent and biofunctionalized nanocrystals," *Nature Nanotechnology*, vol. 4, pp. 121–125, 2009.

[40] I. Ocsoy, M. L. Paret, M. A. Ocsoy et al., "Nanotechnology in plant disease management: DNA-directed silver nanoparticles on graphene oxide as an antibacterial against *Xanthomonas perforans*," *ACS nano*, vol. 7, no. 10, pp. 8972–8980, 2013.

[41] C. T. Wirges, J. Timper, M. Fischler et al., "Controlled nucleation of DNA metallization," *Angewandte Chemie International Edition*, vol. 48, pp. 219–223, 2009.

[42] L. Zhou, Z. Liu, Z. Wang et al., "*Astragalus* polysaccharides exerts immunomodulatory effects *via* TLR4-mediated MyD88-dependent signaling pathway *in vitro* and *in vivo*," *Scientific Reports*, vol. 7, Article ID 44822, 2017.

[43] Y. Leng, L. Fu, L. Ye et al., "Protein-directed synthesis of highly monodispersed, spherical gold nanoparticles and their applications in multidimensional sensing," *Scientific Reports*, vol. 6, Article ID 28900, 2016.

[44] D. Turek, D. Van Simaeys, J. Johnson, I. Ocsoy, and W. Tan, "Molecular recognition of live methicillin-resistant staphylococcus aureus cells using DNA aptamers," *World Journal of Translational Medicine*, vol. 2, no. 3, pp. 67–74, 2013.

[45] P. Wu, T. Zhao, Y. Tian, L. Wu, and X. Hou, "Protein-directed synthesis of Mn-doped ZnS quantum dots: a dual-channel biosensor for two proteins," *Chemistry A European Journal*, vol. 19, no. 23, pp. 7473–7479, 2013.

[46] P. Dam, S. Altuntas, R. Mondal et al., "Silk-based nano-biocomposite scaffolds for skin organogenesis," *Materials Letters*, vol. 327, Article ID 133024, 2022.

[47] A. Demirbas, B. A. Welt, and I. Ocsoy, "Biosynthesis of red cabbage extract directed AgNPs and their effect on the loss of antioxidant activity," *Materials Letters*, vol. 179, pp. 20–23, 2016.

[48] J. Lu, J. Guo, S. Song et al., "Preparation of Ag nanoparticles by spark ablation in gas as catalysts for electrocatalytic hydrogen production," *RSC Advances*, vol. 10, no. 63, pp. 38583–38587, 2020.

[49] C.-B. Qin, X.-L. Liang, S.-P. Han et al., "Giant enhancement of photoluminescence emission in monolayer WS2 by femtosecond laser irradiation," *Frontiers of Physics*, vol. 16, Article ID 12501, 2021.

[50] A. Demirbas, V. Yilmaz, N. Ildiz, A. Baldemir, and I. Ocsoy, "Anthocyanins-rich berry extracts directed formation of AgNPs with the investigation of their antioxidant and antimicrobial activities," *Journal of Molecular Liquids*, vol. 248, pp. 1044–1049, 2017.

[51] E. Dogru, A. Demirbas, B. Altinsoy, F. Duman, and I. Ocsoy, "Formation of *Matricaria chamomilla* extract-incorporated Ag nanoparticles and size-dependent enhanced antimicrobial property," *Journal of Photochemistry and Photobiology B: Biology*, vol. 174, pp. 78–83, 2017.

[52] I. Ocsoy, D. Tasdemir, S. Mazicioglu, C. Celik, A. Katı, and F. Ulgen, "Biomolecules incorporated metallic nanoparticles synthesis and their biomedical applications," *Materials Letters*, vol. 212, pp. 45–50, 2018.

[53] M. Snoussi, E. Noumi, N. Trabelsi, G. Flamini, A. Papetti, and V. De Feo, "Mentha *spicata* essential oil: chemical composition, antioxidant and antibacterial activities against planktonic and biofilm cultures of *Vibrio* spp. strains," *Molecules*, vol. 20, no. 8, pp. 14402–14424, 2015.

[54] P. Barton, R. E. Hughes Jr., and M. M. Hussein, "Supercritical carbon dioxide extraction of peppermint and spearmint," *The Journal of Supercritical Fluids*, vol. 5, no. 3, pp. 157–162, 1992.

[55] B. Marongiu, S. Porcedda, G. D. Porta, and E. Reverchon, "Extraction and isolation of *Salvia desoleana* and *Mentha spicata* subsp. *insularis* essential oils by supercritical CO_2," *Flavour and Fragrance Journal*, vol. 16, no. 5, pp. 384–388, 2001.

[56] J. Pino, P. Borges, M. Martínez et al., "Essential oil of *Mentha spicata* L. from Jalisco," *Journal of Essential Oil Research*, vol. 13, no. 6, pp. 409-410, 2001.

[57] R. Mickienė, O. Ragažinskienė, and B. Bakutis, "Antimicrobial activity of *Mentha arvensis* L. and *Zingiber officinale* R. essential oils," *Biologija*, vol. 57, no. 2, pp. 92–97, 2011.

[58] S. B. Al-Masaudi and S. M. S. Al-Maaqar, "Susceptibility of multidrug-resistant enteric pathogenic diarrheal bacteria to Saudi honey," *Journal of King Abdulaziz University: Science*, vol. 32, no. 1, pp. 47–64, 2020.

[59] NCCLS, *Methods for Dilution Antimicrobial Susceptibility Tests for Bacteria that Grow Aerobically, Approved Standard M7-A7*, Vol. 26, National Committee for Clinical Laboratory Standards, 2009.

[60] M. Elshikh, S. Ahmed, S. Funston et al., "Resazurin-based 96-well plate microdilution method for the determination of minimum inhibitory concentration of biosurfactants," *Biotechnology Letters*, vol. 38, pp. 1015–1019, 2016.

[61] C. Monica, *District Laboratory Practice in Tropical Countries*, Cambridge University Press, Cambridge, 2nd edition, 2005.

[62] S. A. Akintelu, Y. Bo, and A. S. Folorunso, "A review on synthesis, optimization, mechanism, characterization, and antibacterial application of silver nanoparticles synthesized from plants," *Journal of Chemistry*, vol. 2020, Article ID 3189043, 12 pages, 2020.

[63] S. K. Srikar, D. D. Giri, D. B. Pal, P. K. Mishra, and S. N. Upadhyay, "Green synthesis of silver nanoparticles: a review," *Green and Sustainable Chemistry*, vol. 6, pp. 34–56, 2016.

[64] M. A. Nogin ov, G. Zhu, M. Bahoura et al., "Enhancement of surface plasmons in an Ag aggregate by optical gain in a dielectric medium," *Optics Letters*, vol. 31, no. 20, pp. 3022–3024, 2006.

[65] A. Taleb, C. Petit, and M. P. Pileni, "Optical properties of self-assembled 2D and 3D superlattices of silver nanoparticles," *The Journal of Physical Chemistry B*, vol. 102, no. 12, pp. 2214–2220, 1998.

[66] S. Link and M. A. El-Sayed, "Optical properties and ultrafast dynamics of metallic nanocrystals," *Annual Review of Physical Chemistry*, vol. 54, pp. 331–366, 2003.

[67] C. J. Addison and A. G. Brolo, "Nanoparticle-containing structures as a substrate for surface-enhanced raman scattering," *Langmuir*, vol. 22, no. 21, pp. 8696–8702, 2006.

[68] M. Meyer, E. Le Ru, and P. Etchegoin, "Self-limiting aggregation leads to long-lived metastable clusters in colloidal solutions," *The Journal of Physical Chemistry B*, vol. 110, no. 12, pp. 6040–6047, 2006.

[69] P. K. Jain, K. S. Lee, I. H. El-Sayed, and M. A. El-Sayed, "Calculated absorption and scattering properties of gold nanoparticles of different size, shape, and composition: applications in biological imaging and biomedicine," *The Journal of Physical Chemistry B*, vol. 110, no. 14, pp. 7238–7248, 2006.

[70] K. L. Kelly, E. Coronado, L. L. Zhao, and G. C. Schatz, "The optical properties of metal nanoparticles: the influence of size, shape, and dielectric environment," *The Journal of Physical Chemistry B*, vol. 107, no. 3, pp. 668–677, 2003.

[71] W. Zhang, X. Qiao, and J. Chen, "Synthesis and characterization of silver nanoparticles in AOT microemulsion system," *Chemical Physics*, vol. 330, no. 3, pp. 495–500, 2006.

[72] J. Jalab, W. Abdelwahed, A. Kitaz, and R. Al-Kayali, "Green synthesis of silver nanoparticles using aqueous extract of *Acacia cyanophylla* and its antibacterial activity," *Heliyon*, vol. 7, no. 9, Article ID e08033, 2021.

[73] N. Ahmad, S. Sharma, M. K. Alam et al., "Rapid synthesis of silver nanoparticles using dried medicinal plant of basil," *Colloids and Surfaces B: Biointerfaces*, vol. 81, no. 1, pp. 81–86, 2010.

[74] K. Jemal, B. V. Sandeep, and S. Pola, "Synthesis, characterization, and evaluation of the antibacterial activity of *Allophylus serratus* leaf and leaf derived callus extracts mediated silver nanoparticles," *Journal of Nanomaterials*, vol. 2017, Article ID 4213275, 11 pages, 2017.

[75] M.-H. Oh, N.-S. Kim, and S.-M. Kang, "Effect of conductivity of the aqueous solution on the size of printable nanoparticle," *Journal of Nanotechnology*, vol. 2012, Article ID 467812, 4 pages, 2012.

[76] V. S. Suvith and D. Philip, "Catalytic degradation of methylene blue using biosynthesized gold and silver nanoparticles," *Spectrochimica Acta Part A: Molecular and Biomolecular Spectroscopy*, vol. 118, pp. 526–532, 2014.

[77] K. Jeeva, M. Thiyagarajan, V. Elangovan, N. Geetha, and P. Venkatachalam, "*Caesalpinia coriaria* leaf extracts mediated biosynthesis of metallic silver nanoparticles and their antibacterial activity against clinically isolated pathogens," *Industrial Crops and Products*, vol. 52, pp. 714–720, 2014.

[78] S. A. Ahmad, S. S. Das, A. Khatoon et al., "Bactericidal activity of silver nanoparticles: a mechanistic review," *Materials Science for Energy Technologies*, vol. 3, pp. 756–769, 2020.

[79] T. Bruna, F. Maldonado-Bravo, P. Jara, and N. Caro, "Silver nanoparticles and their antibacterial applications," *International Journal of Molecular Sciences*, vol. 22, no. 13, Article ID 7202, 2021.

[80] A. Ivask, A. ElBadawy, C. Kaweeteerawat et al., "Toxicity mechanisms in *Escherichia coli* vary for silver nanoparticles and differ from ionic silver," *ACS Nano*, vol. 8, no. 1, pp. 374–386, 2014.

[81] M. Seong and D. G. Lee, "Silver nanoparticles against *Salmonella enterica* serotype typhimurium: role of inner membrane dysfunction," *Current Microbiology*, vol. 74, no. 6, pp. 661–670, 2017.

[82] S. Agnihotri, S. Mukherji, and S. Mukherji, "Size-controlled silver nanoparticles synthesized over the range 5–100 nm using the same protocol and their antibacterial efficacy," *RSC Advances*, vol. 4, no. 8, pp. 3974–3983, 2014.

[83] P. Korshed, L. Li, Z. Liu, A. Mironov, and T. Wang, "Size-dependent antibacterial activity for laser-generated silver nanoparticles," *Journal of Interdisciplinary Nanomedicine*, vol. 4, no. 1, pp. 24–33, 2019.

[84] A. Ivask, I. Kurvet, K. Kasemets et al., "Size-dependent toxicity of silver nanoparticles to bacteria, yeast, algae, crustaceans and mammalian cells *in vitro*," *PLOS ONE*, vol. 9, no. 7, Article ID e102108, 2014.

[85] B. Le Ouay and F. Stellacci, "Antibacterial activity of silver nanoparticles: a surface science insight," *Nano Today*, vol. 10, no. 3, pp. 339–354, 2015.